Design a Nonlinear Control Using Exact Input-Output Feedback Linearization for CE152 Magnetic Levitation

Hassan S. Al-Nahhal, and Moayed Almobaied

https://doi.org/10.33976/JERT.11.1/2024/1

Abstract—Technological advances necessitate intelligent control rules in order to achieve tight specifications, which underlines the growing importance of nonlinear control systems. A magnetic levitation benchmark is a nonlinear system that's popular among engineers. Because of the considerable nonlinearity in the modelling process of such systems, many researchers in the control engineering field have found analysing the controller's performance to be a challenging experience. The objective of this research is to use an exact input–output feedback linearization approach to develop a control scheme for a magnetic levitation system. This work presents a dynamic magnetically levitated simulations based on the mathematical description of the nonlinear system. The levitation simulation model is incorporated into a control system with the aim of preserving a steady state specified by a desired trajectory, which is simulated by Matlab/Simulink.

Index Terms—CE152 Maglev, exact input–output feedback linearization, nonlinear control, pole-placement.

I. INTRODUCTION

The Magnetic Levitation (Maglev) system is a technique of suspending a target in the air via magnetic force manipulation. This magnetic force is utilized to counteract the target's gravitational force [1]. The magnetic levitation methodology is a well-developed and rapidly expanding technology in which the common denominator in their applications is the absence of touch, resulting in no wear and friction [2]. High-speed trains suspension, superconductor rotor suspension of gyroscopes, rocket-guiding projects, magnetic bearings, and vibration isolation systems are indeed some of several industrial applications for magnetic levitation systems [3-8]. Due to magnetism's highly nonlinear behavior, the mathematical model for magnetic levitation applications is unstable. Hence, there is a considerable need for modeling and control research in industry and academia. Modeling can be accomplished using two approaches: the linearized one and the nonlinear one. For linearized models, techniques such as PI, PID, fuzzy, and state feedback LQR are widely used as in [9-12]. PID is the most common and straightforward of these strategies to create and execute. The greatest drawback of the PID controller is the adjusting procedure for the gains of PID parameters[13] .As an alternative, exact input-output feedback linearization , the sliding mode control using Lyapunov functions represents one of the promising methods for the nonlinear approach [14-16]. The study and formulation of nonlinear systems necessitates knowledge in mathematical disciplines such as differential geometry, etc. However, as computing science progresses, non-linear synthesis procedures are becoming more widely [17]. In this paper will show how to use the exact input-output feedback linearization (FBL) algorithm to obtain a control scheme for a simulation software of magnetic levitation depending on the Humusoft CE152 model of magnetic levitation [18]. The following is a description of how the paper is organized. Section II depicts a mathematical model of the CE152 magnetic levitation system. The state space model of the CE152 magnetic levitation is described by section III. A general explanation of the exact input – output feedback linearization approach is presented in Section IV. In Section V, the exact input-output feedback linearization approach and pole-placement are used to linearize the nonlinear magnetic levitation model. The simulation results are described in section VI to show that the proposed techniques are appropriate. Finally, conclusion observations are addressed in section VII.

II. CE152 MAGNETIC LEVITATION MODELLING SYSTEM

The Magnetic Levitation CE152 demonstrates challenges and difficulties in nonlinear and unstable control systems. Fig.

Figure 1 CE152 magnetic levitation

1 illustrates the Magnetic levitation CE152 model which is comprised of metal ball, coil, PC with Data Acquisition (DAQ) Card and power amplifier [18].

A steel ball is held in a magnetic field which is generated by a current in the coil. The target of the control magnetic levitation system is achieved by balancing the two forces on the ball, the gravity force (downward) and the magnetic force which tries to attract the ball upward [19].

The block diagram of Magnetic Levitation CE152 system is demonstrated by Fig. 2 which consists of:

- Digital-to-Analog converter.
- power amplifier.
- Ball and coil.
- Position sensor.
- Analog-to- Digital converter.

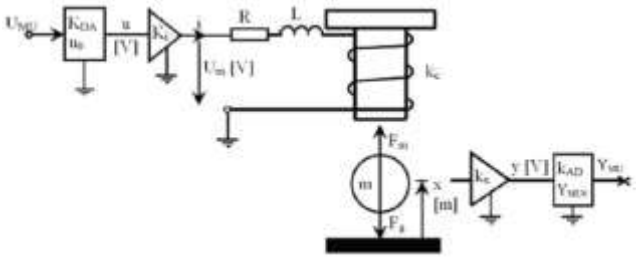

Figure 2 Scheme of the Magnetic levitation CE152 model

A. Digital-to-Analog converter subsystem

D/A converter can be characterized in terms of equation (1) which is represented by Simulink block model as shown in Fig. 3.

$$u = k_{DA}u_{MU} + u_0 \quad (1)$$

Where u is the model output voltage [V], kDA is the D/A converter gain [V/MU], uMU is the D/A converter input [MU] and u0 is the D/A converter offset [V].

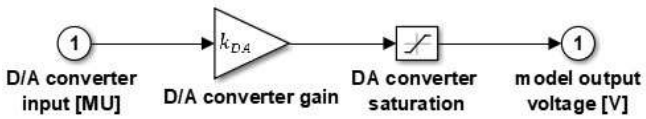

Figure 3 Digital-to-Analog converter subsystem

B. The power amplifier subsystem

Fig. 4 demonstrates the internal structure of the power amplifier which is designed as a source of constant current with the feedback stabilization current.

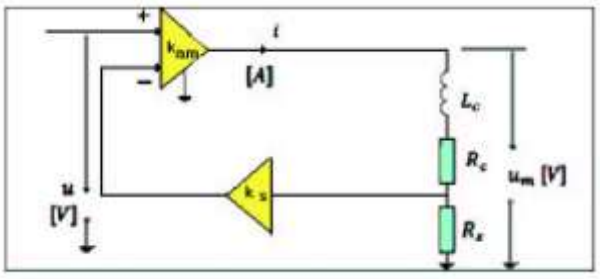

Figure 4 The power amplifier subsystem

Equations (2) and (3) are obtained by applying the Kirchhoff's Voltage Law (KVL) to power amplifier circuit.

$$Um = \frac{L_c di}{dt} + (Rc + Rs)i \quad (2)$$

$$U_m = k_{am}(u - R_s i k_s) \quad (3)$$

The amplifier voltage u and the amplifier current i are considered as the input voltage and the output current of the power amplifier respectively. The transfer function of the power amplifier is illustrated by solving equations (2) and (3) with applying the Laplace transform as following.

$$\frac{I(s)}{U(s)} = \frac{\frac{k_{am}}{(R_c + R_s)+R_s k_s k_{am}}}{\left(\frac{L_c}{(R_c + R_s)+R_s k_s k_{am}} s + 1\right)} \quad (4)$$

The transfer function of the power amplifier can be represented by equation (5).

$$\frac{I(s)}{U(s)} = \frac{k_i}{(T_a s + 1)} \quad (5)$$

Where,

$$k_i = \frac{k_{am}}{(R_c + R_s)+R_s k_s k_{am}} \quad (6)$$

$$T_a = \frac{L_c}{(R_c + R_s)+R_s k_s k_{am}} \quad (7)$$

Where k_i and T_a are called the coil and amplifier gain and the coil and amplifier time constant respectively. The inverse Laplace transform of the current is illustrated by equation (8).

$$i(t) = k_i(1 - e^{-\frac{t}{T_a}}) \quad (8)$$

At T_a is quite little (ms):

$$i(t) = \lim_{T_a \to 0} k_i \left(1 - e^{-\frac{t}{T_a}}\right) = k_i = k_i u(t) \quad (9)$$

C. Ball and Coil Subsystem

The magnetic levitation system is designed to levitate a mass (ball). This will be occurred at the point of equilibrium where there are no forces present as shown in Fig. 5. Lagrange's equations, the model of the ball and coil for magnetic levitation can be described as follows.

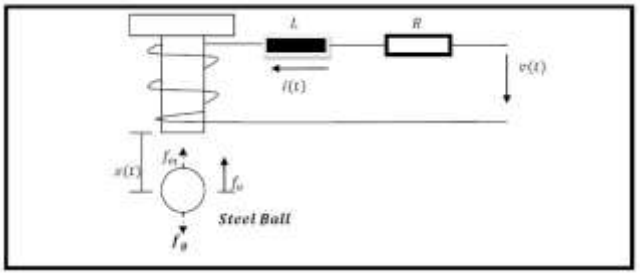

$$\mathcal{L}(x, \dot{x}) = T - V = \frac{1}{2} m\dot{x}^2 - mgx \quad (10)$$

Where, T and V denote the ball's kinetic and potential energy respectively.

In the absence of any non-conservative external forces, Lagrange's equations for the magnetic levitation system is given by equation (11).

$$\frac{d}{dt}\frac{\partial \mathcal{L}}{\partial \dot{x}} - \frac{\partial \mathcal{L}}{\partial x} = m\ddot{x} + mg = 0 \quad (11)$$

There are two forces acting on the system, one of them is the force caused by air damping F_d and the other is the force

Figure 5 Magnetic Levitation Basic Setup

of electromagnetic field F_m which can be obtained as following.

The energy in the coil which has N number of coil turns, l the coil length , μ is the permeability of the coil core, L is the inductance and A is the coil cross section area can be demonstrated by the following equation.

$$W_m = \frac{1}{2} L i^2 \quad (12)$$

$$R = \frac{l}{\mu A} \quad (13)$$

$$L = \frac{N^2}{R} = \frac{\mu A N^2}{l} \quad (14)$$

$$W_m = \frac{\mu A N^2}{2l} i^2 \quad (15)$$

$$F_m = \frac{dW_m}{dl} = \frac{\mu A N^2}{2l^2} i^2 = k_c \frac{i^2}{(x - x_0)^2} \quad (16)$$

Where $k_c = \frac{\mu A N^2}{2}$ is the aggregated coil constant $[N/A]$, i is the coil current $[A]$, x is the distance $[m]$ and x_0 is the coil offset $[m]$.

The force caused by air damping F_d:

$$\mathcal{L}(x, \dot{x}) = T - V = \frac{1}{2} m\dot{x}^2 - mgx \quad (17)$$

Where, k_{FV} is the damping constant $[N.s/m]$. The two forces are appended as following:

$$\frac{d}{dt}\frac{\partial \mathcal{L}}{\partial \dot{x}} - \frac{\partial \mathcal{L}}{\partial x} = F_m + F_d \quad (18)$$

From equations (11), (16) and (17):

$$m_k \ddot{x} + m_k g = k_c \frac{i^2}{(x - x_0)^2} - k_{FV}\dot{x} \quad (19)$$

Where. m_k is the ball mass $[kg]$ and g is the gravity acceleration $[m/s^2]$.

Equation (19)can be arranged as following:

$$m_k \ddot{x} = k_c \frac{i^2}{(x - x_0)^2} - m_k g - k_{FV}\dot{x} \quad (20)$$

By substituting $i = k_i u$ from equation (9):

$$m_k \ddot{x} = k_c \frac{(k_i u)^2}{(x - x_0)^2} - k_{FV}\dot{x} - m_k g \quad (21)$$

$$m_k \ddot{x} = k_f \frac{u^2}{(x - x_0)^2} - k_{FV}\dot{x} - m_k g \quad (22)$$

Where $k_f = k_c k_i^2$ is the aggregated coil constant $[N/A]$.

The ball and coil subsystem of the magnetic levitation model which was represented by equation (20) can be demonstrated by Simulink model as shown in Fig. 6.

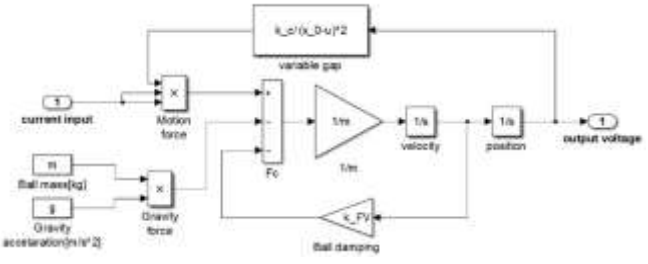

Figure 6 The ball and coil subsystem of the magnetic

D. Position sensor

The position of the ball can be measured by the position

sensor which provides feedback into the system about the ball position. Equation (23) represents the position sensor model.

$$y = k_x x + y_0 \quad (23)$$

Where, y is the model output voltage $[V]$, k_x is the position sensor gain $[V/m]$, x is the ball position $[m]$ and y_0 is position sensor offset $[m]$.

E. Analog-to-Digital converter subsystem

A/D converter can be demonstrated by equation (24).

$$y_{MU} = k_{AD} y + y_{MU0} \quad (24)$$

Where, y_{MU} is the A/D converter output $[V]$, k_{AD} is the D/A converter gain $[MU/V]$, y is the model output voltage $[V]$, and y_{MU0} is the A/D converter offset $[MU]$. Fig. 6 represents the Simulink block diagram of A/D converter and position sensor subsystem.

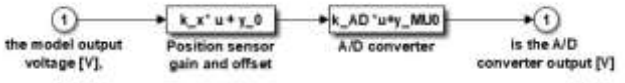

Figure 7 Simulink block diagram of A/D converter and position sensor subsystems

III. CE152 MAGNETIC LEVITATION

STATE SPACE MODEL

The state equations of the CE152 magnetic levitation system can be presented from equations (5) and (20) as shown in equation (24) By supposing $\dot{x}_1 \triangleq x_2 \triangleq \dot{x}$, $i \triangleq x_3$, $A_1 \frac{k_c}{m_k}$, $B_1 = \frac{k_{FV}}{m_k}$, $C_1 = k_{DA} k_i$ and $D_1 = k_{AD} k_x$.

$$\begin{aligned} \dot{x}_1 &= x_2 \\ \dot{x}_2 &= A_1 \frac{x_3^2}{(x_1 - x_0)^2} - B_1 x_2 - g \\ \dot{x}_3 &= -\frac{1}{T_a} x_3 + \frac{C_1}{T_a} u \\ y &= D_1 x_1 \end{aligned} \quad (24)$$

The nonlinearity of the system is demonstrated by the state space model in the foregoing equations. The system can be controlled in two main methods: linear system control and nonlinear system control. The study and formulation of nonlinear systems necessitates knowledge in mathematical disciplines such as differential geometry, etc. However, as computing science progresses, non-linear synthesis procedures are becoming more widely used[17]. The exact input-output feedback linearization technique will be discussed by the following sections, and the controllers for the CE152 magnetic levitation benchmark will be simulated. Table 1 demonstrates the CE152 Maglev parameters which are used in modelling of the system.

IV. EXACT INPUT-OUTPUT FEEDBACK LINEARIZATION

This section will show how to use the exact input-output feedback linearization (FBL) algorithm to obtain a control scheme for a simulation software of magnetic levitation depending on the Humusoft CE 152 model of magnetic levitation[20]. This technique is premised on the theory of compensating for nonlinear effects in the system by adding dynamical controller, culminating in a system that behaves linearly in regard to the proposed input $v(t)$ and $y(t)$ as output of the system[21].

Equation (25) demonstrates the formula of the nonlinear system.

$$\begin{aligned} \dot{x}(t) &= f(x) + g(x)u(t) \\ y(t) &= h(x \end{aligned} \quad (25)$$

Where $x(t) \in R^n$ is state vector, u(t) is input control, y(t) is the output of the system, $f(x)$, $g(x)$ and $h(x)$ are nonlinear functions.

TABLE 1 CE152 Maglev model parameters.

Parameter	Symbol	Value
ball mass [kg]	mk	0.0084
viscose friction[unitless]	KFv	0.02
ball diameter [m]	Dk	12.7e-3
gravity acceleration constant $[m.s^{-2}]$	g	9.81
maximum DA converter output voltage[unitless]	U_DAm	5
coil resistance [Ohm]	Rc	3.5
coil inductance [H]	Lc	30e-3
current sensor resistance [Ohm]	R_s	0.25
current sensor gain [unitless]	k_s	13.33
power amplifier gain [unitless]	K_am	100
maximum power amplifier output current[A]	I_am	1.2
amplifier time constant [s]	Ta	1.8694e-05
amplifier gain [A/V]	k_i	0.2967
D/A converter gain[unitless]	k_DA	10
A/D converter gain[unitless]	k_AD	0.2
position sensor constant[unitless]	k_x	797.4603
aggregated coil constant[N/V]	k_f	0.606e-6
coil constant[unitless]	k_c	6.8823e-06
coil limit bias [m]	x_0	8.26e-3

The exact input–output feedback linearization approach is created by computing the differentiation of the output of the system $y(t)$till it becomes proportional to the input $u(t)$.The number of derivations defines the system's relative order r [17].

Linearization stages for the nonlinear system (24) using the exact input–output feedback linearization approach are as flowchart in the Fig. 8.

V. NONLINEAR CONTROL

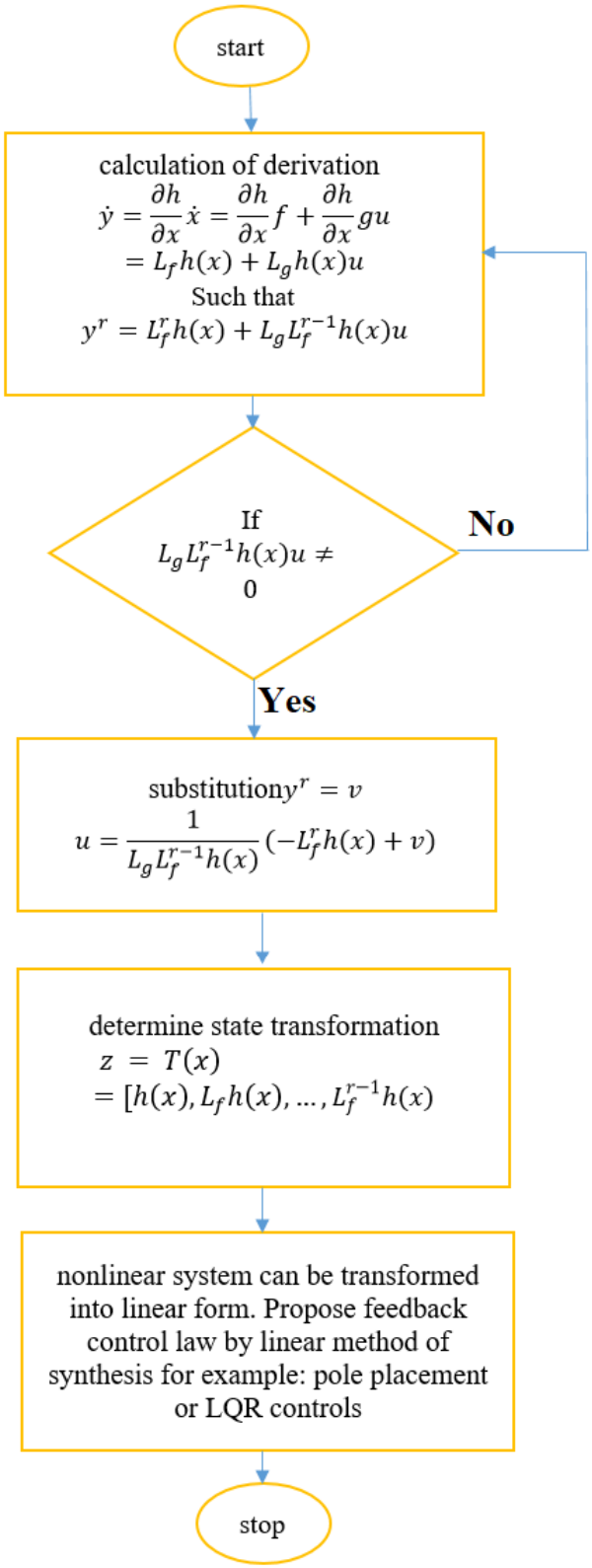

ALGORITHM DESIGN USING EXACT INPUT-OUTPUT FEEDBACK LINEARIZATION

This section provides a exact input-output feedback linearization mechanism for the nonlinear maglev model and designs a control scheme for the resulting model. Suppose the state state space form of the Magnetic levitation in the equation (24). The derivative of the system output y is then applied until there is a dependency on the input u:

$$\begin{aligned} \boldsymbol{y} &= \boldsymbol{D_1 x_1} \\ \boldsymbol{\dot{y}} &= \boldsymbol{D_1 \dot{x}_1 = D_1 x_2} \\ \boldsymbol{\ddot{y}} &= \boldsymbol{D_1 \dot{x}_2 = D_1 (A_1 \frac{x_3^2}{(x_1 - x_0)^2} - B_1 x_2 - g)} \\ \boldsymbol{\ddot{y}} &= \boldsymbol{f(x) + g(x)u} \end{aligned} \tag{26}$$

The following calculations can be used to determine $f(x)$ and $g(x)$.

$$\boldsymbol{\ddot{y} = D_1 \left(-B_1 \dot{x}_2 - \frac{2A_1 x_3^2 \dot{x}_1}{(x_1 - x_0)^3} + \frac{2A_1 x_3 \dot{x}_3}{(x_1 - x_0)^2} \right)} \tag{27}$$

Equation (27) can rearrange as following:

$$\begin{aligned} \boldsymbol{\ddot{y}} = &\boldsymbol{\frac{2A_1 D_1 x_3^2 x_2}{(x_0 - x_1)^3} + D_1 B_1 \left(A_1 \frac{x_3^2}{(x_0 - x_1)^2} \right.} \\ &\boldsymbol{\left. - B_1 x_2 - g \right)} \\ &\boldsymbol{- \frac{2A_1 D_1 x_3^2}{T_a (x_0 - x_1)^2}} \\ &\boldsymbol{+ \frac{2A_1 D_1 C_1 x_3}{(x_0 - x_1)^2} u} \end{aligned} \tag{28}$$

Where,

$$\begin{aligned} \boldsymbol{f(x)} = &\boldsymbol{\frac{2A_1 D_1 x_3^2 x_2}{(x_0 - x_1)^3}} \\ &\boldsymbol{+ D_1 B_1 \left(A_1 \frac{x_3^2}{(x_0 - x_1)^2} \right.} \\ &\boldsymbol{\left. - B_1 x_2 - g \right)} \\ &\boldsymbol{- \frac{2A_1 D_1 x_3^2}{T_a (x_0 - x_1)^2}} \end{aligned} \tag{29}$$

$$\boldsymbol{g(x) = \frac{2A_1 D_1 C_1 x_3}{(x_0 - x_1)^2}} \tag{30}$$

After substitution $\ddot{y} = v$, the resulting input transformation has following form:

Figure 8 Flowchart of exact input – output feedback linearization method

$$u = \frac{1}{g(x)}(-f(x) + v) \tag{31}$$

The corresponding state transformation z = T (x) can be determined as shown in equation (32).

$$\begin{bmatrix} z_1 \\ z_2 \\ z_3 \end{bmatrix} = \begin{bmatrix} y = D_1 x_1 \\ \dot{y} = D_{1x_2} \\ \ddot{y} = D_1 \dot{x}_2 \end{bmatrix} \tag{32}$$

After that, the nonlinear system is transformed into linear system as it is demonstrated by the equation (33).

$$\begin{bmatrix} \dot{z}_1 \\ \dot{z}_2 \\ \dot{z}_3 \end{bmatrix} = \begin{bmatrix} 0 & 1 & 0 \\ 0 & 0 & 1 \\ 0 & 0 & 0 \end{bmatrix} \begin{bmatrix} z_1 \\ z_2 \\ z_3 \end{bmatrix} + \begin{bmatrix} 0 \\ 0 \\ 1 \end{bmatrix} v \tag{33}$$

Where,

$$v = -Kz + K_o y_{ref} \tag{34}$$

Where $K = [k_1, k_2. k_3]$ is the vector gains.

The resulting input transformation in equation (32), state transformation in equation (33) and the control law in equation (34) are established by simulation of Simulink in matlab which is displayed by the Fig. 9 .

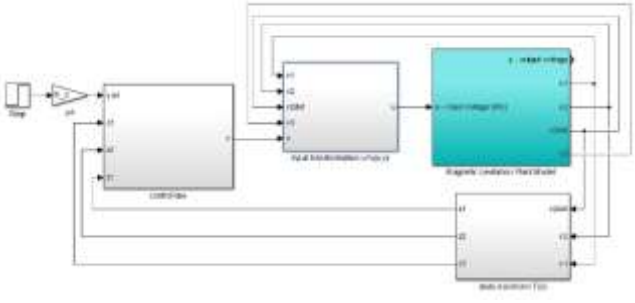

Figure 9 The Simulink of the nonlinear model for Maglev

The state feedback control equation was constructed in the form of equation (34). Depending on the vector of the dynamical system (32), properly chosen roots [k1, k2.k3] using the pole – placement method. Equation (35) illustrates the new linear system.

$$\begin{bmatrix} \dot{z}_1 \\ \dot{z}_2 \\ \dot{z}_3 \end{bmatrix} = \begin{bmatrix} 0 & 1 & 0 \\ 0 & 0 & 1 \\ -k_1 & -k_2 & -k_3 \end{bmatrix} \begin{bmatrix} z_1 \\ z_2 \\ z_3 \end{bmatrix} + \begin{bmatrix} 0 \\ 0 \\ K_o \end{bmatrix} y_{ref} \tag{35}$$

The characteristic polynomial for the system in equation (35) becomes as follows:

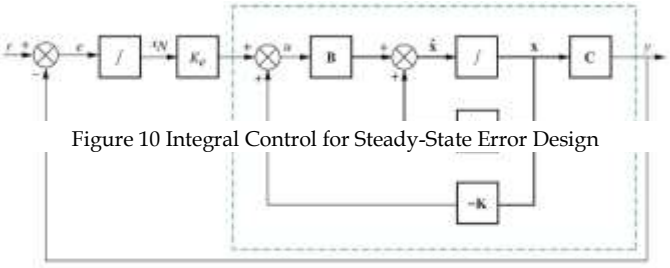

Figure 10 Integral Control for Steady-State Error Design

$$\begin{aligned} P(S) &= det(SI - A) \\ &= \begin{vmatrix} -S & 1 & 0 \\ 0 & -S & 1 \\ -k_1 & -k_2 & -k_3 - S \end{vmatrix} \\ &= S^3 + k_3 S^2 + k_2 S + k_1 \end{aligned} \tag{36}$$

An integral state feedback controller will be constructed to eliminate the steady state error as shown in Fig. 10.

The state space model can be modified to become as follows.

$$\begin{bmatrix} \dot{z} \\ \dot{z_N} \end{bmatrix} = \begin{bmatrix} A & BK_e \\ -C & 0 \end{bmatrix} \begin{bmatrix} z \\ z_N \end{bmatrix} + \begin{bmatrix} 0 \\ 1 \end{bmatrix} r$$
$$y = [C \quad 0] \begin{bmatrix} z \\ z_N \end{bmatrix} \tag{37}$$

The linear system in equation (35) can be rewritten as the form in equation (37) as follows:

$$\begin{bmatrix} \dot{Z}_1 \\ \dot{Z}_2 \\ \dot{Z}_3 \\ \dot{Z_N} \end{bmatrix} = \begin{bmatrix} 0 & 1 & 0 & 0 \\ 0 & 0 & 1 & 0 \\ K_1 & K_2 & K_3 & K_e \\ -1 & 0 & 0 & 0 \end{bmatrix} \begin{bmatrix} Z_1 \\ Z_2 \\ Z_3 \\ Z_N \end{bmatrix} + \begin{bmatrix} 0 \\ 0 \\ 0 \\ 1 \end{bmatrix} r$$
$$y = [1 \quad 0 \quad 0 \quad 0] \begin{bmatrix} Z_1 \\ Z_2 \\ Z_3 \\ Z_N \end{bmatrix} \tag{38}$$

Where the closed loop system characteristic polynomial representing a 4th order system:

$$P(S) = S^4 + k_1 S^3 + k_2 S^2 + k_3 S + K_e \tag{39}$$

If the settling time is equal to 0.5s and the percentage of overshoot is 0% then, the damping ratio and natural frequency

$\zeta = 1$, $\omega_n = 8$ for an estimated second-order system with dominant poles at $P_{1,2} = -\zeta\omega_n \pm \omega_n\sqrt{1-\zeta} = -8$ conform to the requirements. Place the 3rd and 4th poles at minimum 10 times the distance between them and the dominant poles. The characteristic polynomial will be as following:

$$P(S) = (S+8)^2(S+80)(S+800) = S^4 + 896S^3 + 78144S^2 + 1080320S + 4096000 \quad \textbf{(40)}$$

By comparing the two equations (39) and (40) the gains for the control are as shown in equation (41).

$$\boldsymbol{K} = \begin{bmatrix} k_1 \\ k_2 \\ k_3 \\ k_e \end{bmatrix}^{\boldsymbol{T}} = \begin{bmatrix} 896 \\ 78144 \\ 1080320 \\ 4096000 \end{bmatrix}^{\boldsymbol{T}} \quad \textbf{(41)}$$

VI. RESULTS AND SIMULATION

Applying the mechanisms shown by Fig. 9 and the gains of the controller in the equation (41). Exact Input-Output Feedback Linearization with Pole placement technique is used to determine the relevant position, velocity, and acceleration signals. The estimated position, velocity, and current signals are shown in Fig. 11, which demonstrates that the controllers satisfied their positional objective in 0.5 seconds. These observations strongly suggest that the control system is capable for estimating displacement, velocity, and acceleration for use as feedback signals in motion - based applications.

Fig. 12 illustrates the step response for the Exact input–output feedback linearization (EIOFL) and the PID controller when the PID gains controller are ($K_P = 1, K_I = 2000, K_D = 5$). The results show that the proposed controller using (EIOFL) controller outperformed PID controller. Table 2 listed the Performance comparison between EIOFL and PID controllers.

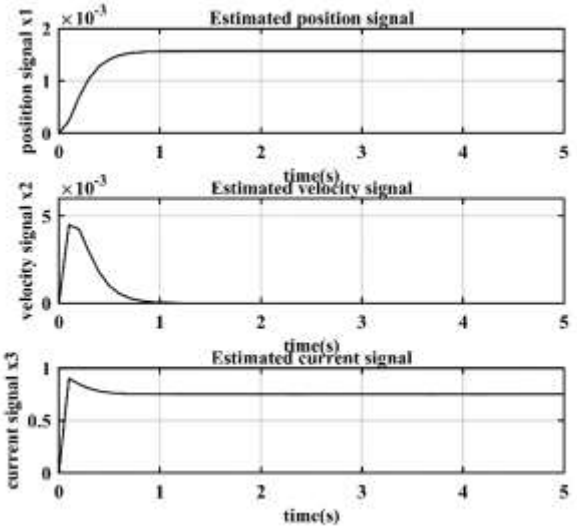

Figure 12 Estimated position,velocity and current signals

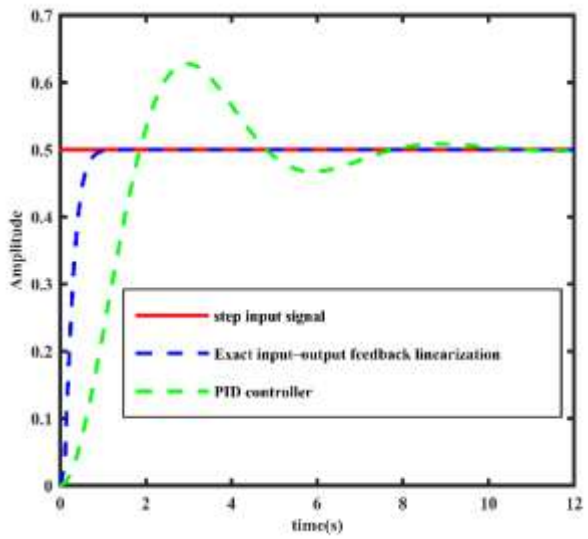

Figure 13 Output step response for the Exact input–output feedback linearization (EIOFL) and the PID controllers

The tracking accuracy for a sinusoidal input command signal is similarly adequate. In addition, at time point $t = 0sec, t = 10sec$, $t = 20sec, t = 30$, and $t = 40sec$, we purposefully add an impulsive signal to evaluate its robustness against impulse perturbations. The suggested technique proves to be robust to shocks as shown in Fig. 13. Finally, according to simulation results, the Exact Input-Output Feedback Linearization technique can develop a closed-loop control system with good tracking performance.

table 2 Performance comparison between EIOFL and PID controllers

Item	EIOFL	PID
Rise time (seconds)	0.1	2.1
Settling time (seconds)	0.3	2.3
Overshot (%)	0	26
Peak amplitude	0.5	3
steady state error	0	0

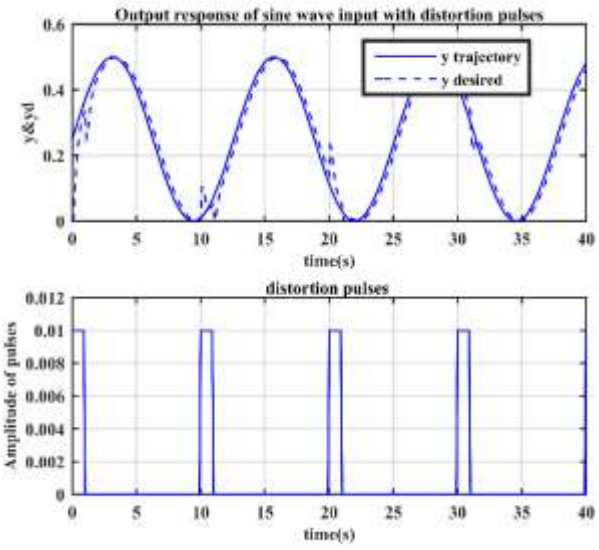

VII. CONCLUSION

The proposed Exact Input-Output Feedback Linearization with Pole Placement technique has been shown to be effective in motion - based applications where motion, speed, and current are frequently required as feedback signals. In this paper, the magnetic levitation system CE152 was employed to illustrate the effectiveness of the suggested control strategy through simulation. According to simulation results, the Exact Input-Output Feedback Linearization technique can develop a closed-loop system with good tracking performance. The control design for a real model of maglev and the support of instruction in the topic of optimal and nonlinear systems will both utilize the information obtained from the field of techniques of synthesis of nonlinear systems in the future.

REFERENCES

[1] M. Ahmed, M. F. Hossen, M. E. Hoque, O. Farrok, and M. Mynuddin, "Design and construction of a magnetic levitation system using programmable logic controller," *American Journal of Mechanical Engineering,* vol. 4, no. 3, pp. 99-107, 2016.

[2] H. Yaghoubi, "The most important maglev applications," *Journal of Engineering,* vol. 2013, 2013.

[3] N. J. Dahlen, "Magnetic active suspension and Isolation," Massachusetts Institute of Technology, Department of Mechanical Engineering, 1985.

[4] J. R. Downer, "Analysis of a single axis magnetic suspension system," Massachusetts Institute of Technology, 1980.

[5] M. Dussaux, "Status of the industrial applications of the active magnetic bearings technology," in *Turbo Expo: Power for Land, Sea, and Air*, 1990, vol. 79085: American Society of Mechanical Engineers, p. V005T14A016.

[6] B.-Z. Kaplan and D. Regev, "Dynamic stabilization of tuned-circuit levitators," *IEEE Transactions on Magnetics,* vol. 12, no. 5, pp. 556-559, 1976.

[7] D. Limbert, H. Richardson, and D. Wormley, "Controlled dynamic characteristics of ferromagnetic vehicle suspensions providing simultaneous lift and guidance," 1979.

[8] J. Paddison, C. Macleod, and R. Goodall, "State variable constraints on the performance of optimal Maglev suspension controllers," in *Control Applications, 1994., Proceedings of the Third IEEE Conference on*, 1994, pp. 599-604.

[9] B. Hamed and H. Abu Elreesh, "Design of optimized fuzzy logic controller for magnetic levitation using genetic algorithms," *Journal of Information and Communication Technologies,* vol. 2, no. 1, 2012.

[10] T.-E. Lee, J.-P. Su, and K.-W. Yu, "Implementation of the state feedback control scheme for a magnetic levitation system," in *2007 2nd IEEE Conference on Industrial Electronics and Applications*, 2007: IEEE, pp. 548-553.

[11] D. Maji, M. Biswas, A. Bhattacharya, G. Sarkar, T. K. Mondal, and I. Dey, "Maglev system modeling and lqr controller design in real time simulation," in *2016 International Conference on Wireless Communications, Signal Processing and Networking (WiSPNET)*, 2016: IEEE, pp. 1562-1567.

[12] S. K. Pandey and V. Laxmi, "PID control of magnetic levitation system based on derivative filter," in *2014 Annual International Conference on Emerging Research Areas: Magnetics, Machines and Drives (AICERA/iCMMD)*, 2014: IEEE, pp. 1-5.

[13] M. Almobaied, H. S. Al-Nahhal, and K. B. Issa, "Computation Of Stabilizing PID Controllers For Magnetic Levitation System With Parametric Uncertainties," in *2021 International Conference on Electric Power Engineering–Palestine (ICEPE-P)*, 2021: IEEE, pp. 1-7.

[14] I. Ahmad and M. A. Javaid, "Nonlinear model & controller design for magnetic levitation system," *Recent advances in signal processing, robotics and automation,* pp. 324-328, 2010.

[15] N. Al-Muthairi and M. Zribi, "Sliding mode control of a magnetic levitation system," *Mathematical problems in engineering,* vol. 2004, no. 2, pp. 93-107, 2004.

[16] X. Shi and Q. Mao, "Research on Control Strategy of

Magnetic Levitation Gravity Compensator Based on Lyapunov Stability Criterion," in *IOP Conference Series: Materials Science and Engineering*, 2018, vol. 452, no. 4: IOP Publishing, p. 042146.

[17] P. Šuster and A. Jadlovska, "Modeling and control design of magnetic levitation system," in *2012 IEEE 10th International Symposium on Applied Machine Intelligence and Informatics (SAMI)*, 2012: IEEE, pp. 295-299.

[18] D. Honc, "Modelling and identification of magnetic levitation model CE 152/revised," in *Computer Science On-line Conference*, 2018: Springer, pp. 35-43.

[19] S. A. El Najjar, "Ripple Free Deadbeat Control for Nonlinear Systems with Time-Delays And Disturbances," 2013.

[20] "Humusoft Praha,CE 512 Education Manual Magnetic Levitation Model," ed.

[21] J.-J. E. Slotine and J. Karl Hedrick, "Robust input-output feedback linearization," *International Journal of control,* vol. 57, no. 5, pp. 1133-1139, 1993.

Hassan S. Al-Nahhal was born on July 28, 1989, in Rafah, Palestine. He received a Bachelor degree in Electrical Engineering from the Islamic University of Gaza in 2012, Also he was studying M.S degree in Control and Communications Systems from the same university. His current researches are on robust control systems, robotics control system, and nonlinear control systems.

Moayed Almobaied is an assistant professor of Electrical Engineering at the Islamic University of Gaza, Palestine. He received his B.Sc and M.Sc degrees in Control Engineering from the Islamic University of Gaza in 2001 and 2008, respectively. In 2017, he received Ph.D. in control and automation systems from Istanbul Technical University. He has received several fellowships including YTB and DAAD. His current research interests include robust control, optimal control, designing of modern control systems, nonlinear control systems, and robotics.